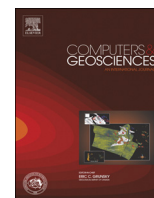




ELSEVIER

Contents lists available at ScienceDirect

Computers & Geosciences

journal homepage: www.elsevier.com/locate/cageo

Case study

Automating the selection of standard parallels for conic map projections

Bojan Šavrič^{a,b,*}, Bernhard Jenny^{a,c}^a College of Earth, Ocean, and Atmospheric Sciences, Oregon State University, Corvallis, OR, USA^b Esri Inc., Redlands, CA, USA^c School of Science, RMIT University, Melbourne, Australia

ARTICLE INFO

Article history:

Received 10 May 2015

Received in revised form

29 September 2015

Accepted 26 February 2016

Available online 3 March 2016

Keywords:

Standard parallels

Conic map projections

Albers conic projection

Lambert conic projection

Equidistant conic projection

Adaptive composite map projections

ABSTRACT

Conic map projections are appropriate for mapping regions at medium and large scales with east–west extents at intermediate latitudes. Conic projections are appropriate for these cases because they show the mapped area with less distortion than other projections. In order to minimize the distortion of the mapped area, the two standard parallels of conic projections need to be selected carefully. Rules of thumb exist for placing the standard parallels based on the width-to-height ratio of the map. These rules of thumb are simple to apply, but do not result in maps with minimum distortion. There also exist more sophisticated methods that determine standard parallels such that distortion in the mapped area is minimized. These methods are computationally expensive and cannot be used for real-time web mapping and GIS applications where the projection is adjusted automatically to the displayed area. This article presents a polynomial model that quickly provides the standard parallels for the three most common conic map projections: the Albers equal-area, the Lambert conformal, and the equidistant conic projection. The model defines the standard parallels with polynomial expressions based on the spatial extent of the mapped area. The spatial extent is defined by the length of the mapped central meridian segment, the central latitude of the displayed area, and the width-to-height ratio of the map. The polynomial model was derived from 3825 maps—each with a different spatial extent and computationally determined standard parallels that minimize the mean scale distortion index. The resulting model is computationally simple and can be used for the automatic selection of the standard parallels of conic map projections in GIS software and web mapping applications.

© 2016 Elsevier Ltd. All rights reserved.

1. Introduction

Conic map projections with a normal aspect show meridians as straight, radiating lines and parallels as concentric arcs. They are used to map regions at medium and large scales with greater east–west extents than north–south extents at intermediate latitudes. In these cases, conic projections have advantageous distortion properties (minimizing distortion) and the directions of the meridians indicate the location of the nearest pole. The Albers equal-area and Lambert conic projections are suggested for mapping a continent, ocean, or smaller region in Snyder's selection guide (Snyder, 1987), which is the most sophisticated and generally recommended map projection selection guideline currently available. Conic projections with carefully selected standard parallels minimize variations in the distortion of the mapped area. Rules of

thumb exist for placing the standard parallels (Bugayevskiy and Snyder, 1995; Maling, 1960, 1992; Snyder, 1987) and they are discussed in the following section. The standard parallels can also be defined with more sophisticated methods. For example, Adams selected standard parallels for the 48 conterminous United States by minimizing the distortion values at the center and along the borders of the map for the Albers equal-area projection (Deetz and Adams, 1934, p. 91; Snyder, 1987). Another example is the work done by Kavrayskiy, who used a least-square error in scale distortion to determine standard parallels for the equidistant conic projection for mapping the European part of the Soviet Union (Maling, 1960, p. 242; Snyder, 1987).

Such sophisticated and computationally expensive methods are not applicable when the standard parallels have to be selected on the fly, for example, in web maps where the map user can change the displayed spatial extent by panning or zooming, or by adjusting the width-to-height ratio of the map. The computations would take too long and prevent smooth interactions on a web map. Instead, the few existing web maps with adaptive composite map projections use rules of thumb to select standard parallels for

* Corresponding author at: College of Earth, Ocean, and Atmospheric Sciences, Oregon State University, Corvallis, OR, USA.

E-mail address: savricb@onid.orst.edu (B. Šavrič).

conic projections. For example, Jenny (2012) places standard parallels at one-sixth of the angular length of the mapped central meridian segment from the upper and lower map borders. This rule of thumb was suggested by Deetz and Adams (1934, p. 79, 91), as discussed further in the next section. Such rules of thumb simplify the selection of standard parallels, but do not generally select the optimal standard parallels to minimize map distortion.

The main objective of the research presented in this article is to develop a mathematical model for selecting the standard parallels of conic projections based on the spatial extent of the mapped area. This model is to be used for selecting standard parallels when the projection is selected on the fly in a web map, GIS, and other geospatial software with adaptive projections. The development idea is to first create a systematic variety of mapping scenarios using three parameters that define the spatial extent of the mapped area: the length of the mapped central meridian segment, the central latitude of the displayed area, and the width-to-height ratio of the map. The standard parallels are determined to minimize the scale distortion for each scenario. From the results of this distortion analysis, a simple mathematical model is derived that returns the optimal standard parallels for a given spatial extent of a map.

This article first documents the existing recommendations and rules of thumb for placing the standard parallels of conic projections. In the Section 3, the parameters of the spatial map extent, the mapping scenarios, the distortion measure used, the computation of optimal standard parallels, and the derivation of the mathematical model are explained. The Section 4 presents the polynomial model defining standard parallels for the three conic projections, documents the evaluation of the model, and details the implementation steps for using the model. In the conclusion, the major advantages of the model are pointed out and possible applications are given. This article has one Appendix, which details the partial derivatives of the three conic projections used for computing the distortion parameters.

2. Existing recommendations

In the past, a few rules of thumb have been suggested for selecting standard parallels for conic projections. The equatorial (or lower) and polar (or upper) standard parallels can be determined using the following simple formulas:

$$\phi_1 = \phi_{\min} + \frac{\phi_{\max} - \phi_{\min}}{K}, \quad \phi_2 = \phi_{\max} - \frac{\phi_{\max} - \phi_{\min}}{K} \quad (1)$$

where ϕ_1 is the equatorial parallel, ϕ_2 is the polar parallel, ϕ_{\max} is the maximum latitude of the mapped central meridian segment, ϕ_{\min} is the minimum latitude of the mapped central meridian segment, and K is a constant (Bugayevskiy and Snyder, 1995; Maling, 1992). Fig. 1 illustrates the parameters for Eq. (1). For the southern hemisphere, the equatorial parallel is computed by subtracting the fraction with constant K from the maximum latitude ϕ_{\max} . The polar parallel is computed by adding the fraction with constant K to the minimum latitude ϕ_{\min} .

Hinks (1912, p. 87) suggested $K = 7$, which places the standard parallels at one-seventh of the length of the mapped central meridian segment from the maximum and minimum latitude of the mapped central meridian segment (Fig. 1). Deetz and Adams (1934, p. 79, 91) suggested $K = 6$. Both of the above suggestions assume that the mapped area completely fills the fan-shape (Fig. 1) (Maling, 1992, p. 242), while most maps (including web maps) have a rectangular shape. The value of the constant K does not change with the spatial extent of the area to be mapped.

According to Bugayevskiy and Snyder (1995) and Maling (1960, 1992), in 1934 Kavrayskiy suggested four K values for mapping

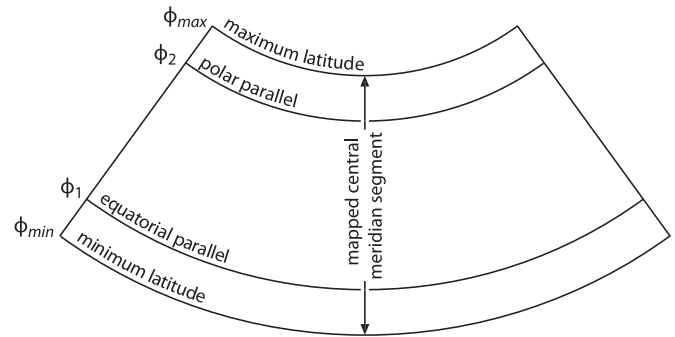


Fig. 1. The fan-shape of the mapped area defined by the maximum and minimum latitude of the mapped central meridian segment with both standard parallels.

areas with different extents: (1) $K = 7$ for areas with a larger extent in longitude, (2) $K = 5$ for areas with a larger extent in latitude, (3) $K = 4$ for areas with circular or elliptical outlines, and (4) $K = 3$ for areas with square outlines. Kavrayskiy's K values assume that the area to be mapped is symmetrical along the central meridian and central latitude. The different K constants improve the models suggested by Deetz and Adams (1934), and Hinks (1912), because they take the shape of the area to be mapped into consideration. However, descriptions of Kavrayskiy's constants are vague, and the shape of the mapped area changes when the area is projected. In addition, the area of interest to be mapped can also be asymmetrical relative to the central latitude and longitude.

One way to improve Kavrayskiy's model and take different asymmetric distributions of the area into account is by applying different values to each of the standard parallels. Hrvatin (2011) used this "double criterion" for defining standard parallels for mapping continents with the Albers equal-area projection. For each part of the mapped area above and below the central latitude, he defined a constant value that matched best with Kavrayskiy's descriptions of the area and used it to compute the standard parallels.

Kavrayskiy's constant values and Hrvatin's "double criterion" take into account the shape of the area being mapped. However, none of the existing models take both the shape and the central latitude of the mapped area into consideration.

3. Methods

To derive a mathematical model for the automated selection of standard parallels, different mapping scenarios were analyzed for the Albers equal-area conic, the Lambert conformal conic, and the equidistant conic projections. For each projection, the optimal standard parallels were computed first for each mapping scenario. Those optimal standard parallels were later used as a basis to define approximating models using polynomial equations. The resulting models—one for each of the three projections—return standard parallels according to the length of the mapped central meridian segment, the central latitude, and the width-to-height ratio of the map. This section details the derivation of the mathematical model.

3.1. Parameters of the spatial map extent and their ranges

To define the extent of the area displayed on the map, three parameters are used: the length of the mapped central meridian segment, the central latitude of the displayed area, and the width-to-height ratio of the map (Fig. 2). These three parameters represent the input variables for the mathematical models presented

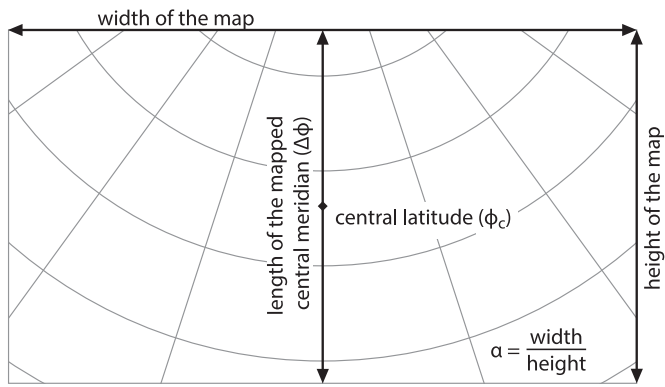


Fig. 2. Input variables for the mathematical model: width and height of the width-to-height ratio (α), the length of the mapped central meridian ($\Delta\phi$), and the central latitude (ϕ_c) of the area to be mapped.

in this article. For the purposes of this article, the term *the length of the mapped central meridian* refers to the parameter defining the length of the mapped central meridian segment in angular units.

Conic projections are appropriate for large-scale maps (Snyder, 1987), therefore we limit the maximum possible length of the mapped central meridian in our model to 45° . The minimum length of the central meridian is 2.5° in our model.

Snyder (1987) suggests conic projections for areas away from the equator. Central latitudes between 15° and 75° are used for our model.

Our model uses map width-to-height ratios between 1 and 3. A width-to-height ratio of 1 represents an equal extent, and azimuthal projections would be more appropriate to use in this case. A width-to-height ratio of 3 results in a map that has a small latitudinal, but large longitudinal extent. When the length of the mapped central meridian is large, a width-to-height ratio of 3 can result in a mapping scenario where a medium-scale projection, e.g. an azimuthal projection, would be more appropriate.

3.2. Mapping scenarios

A total of 425 scenarios for each possible width-to-height ratio were created by varying the maximum and minimum latitude values of the mapped central meridian segment for every 2.5° . In total, 9 width-to-height ratios were used in the analysis: 1, 1.25, 1.5, 1.75, 2, 2.25, 2.5, 2.75, and 3. Altogether, 3825 different mapping scenarios were created for each of the three conic projections. Fig. 3 shows the lengths of the mapped central meridians and central latitudes for one of the width-to-height ratios that was used in the analysis. The top right corner of the graph excludes a few examples, since the northern latitude of their mapped central meridians exceeded 90° .

3.3. Distortion measure

To find the optimum standard parallels for each mapping scenario, a distortion measure is needed. For the purposes of this research, Canters and Declair's (1989) weighted mean error in the overall scale distortion D_{ab} after Canters (2002) was used (Eq. (2)).

$$D_{ab} = \frac{1}{S} \sum_{i=1}^k \left(\frac{a_i^q + b_i^r}{2} - 1 \right) \cos(\phi_i) \Delta\phi \Delta\lambda \quad (2)$$

Eq. (2) computes the index D_{ab} by summing the weighted scale distortion for k sample points. The latitude of a sample point is ϕ_i , and the maximum and minimum scale distortions at the sample point are a_i and b_i . The sum of all area weight factors is computed with $S = \sum_{i=1}^k P_i \cos \phi_i$. P_i equals 1 if the sample point is located

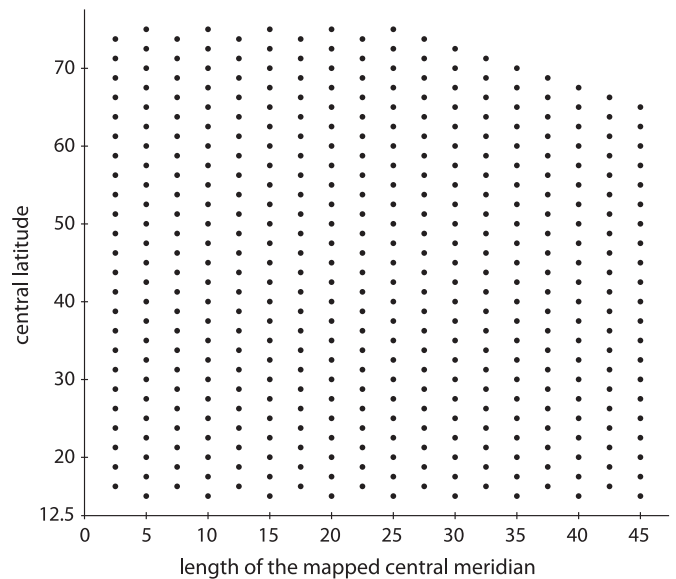


Fig. 3. The lengths of the mapped central meridians and central latitudes for 425 mapping scenarios. The same scenarios were used for all 9 width-to-height ratios.

inside the mapped area; otherwise P_i equals 0. The coefficients q and r are $q = \begin{cases} 1 & a_i \geq 1 \\ -1 & a_i < 1 \end{cases}$, $r = \begin{cases} 1 & b_i \geq 1 \\ -1 & b_i < 1 \end{cases}$.

Canters and Declair (1989) introduced this distortion measure for comparing small-scale projections (Canters, 2002). In other research, this index is used for comparing projections, for example, Jenny et al. (2008, 2010) evaluate projections designed in Flex Projector, Šavrič and Jenny (2014) compare pseudocylindrical projections, and Jenny et al. (2015) analyze cylindrical projections for world maps. Mulcahy (2000) uses a similar index by Canters and Declair (1989) with maximum angular distortion instead of scale distortion for evaluating pixel changes while projecting the global raster data. Using the factor P_i , one can restrict the distortion measure to an area of interest (Canters, 2002). To compute the weighted mean error in the overall scale distortion, only sample points that are inside of the mapped area in each scenario were used.

A regular grid of sample points was defined using the same interval for the latitude and longitude. The interval was computed separately, based on the length of the mapped central meridian for each mapping scenario. 50 rows of sample points, where the central meridian is placed in-between the two central columns of points, were used for the purposes of this study. Fig. 4 shows an example of a regular grid with 5 rows of sample points.

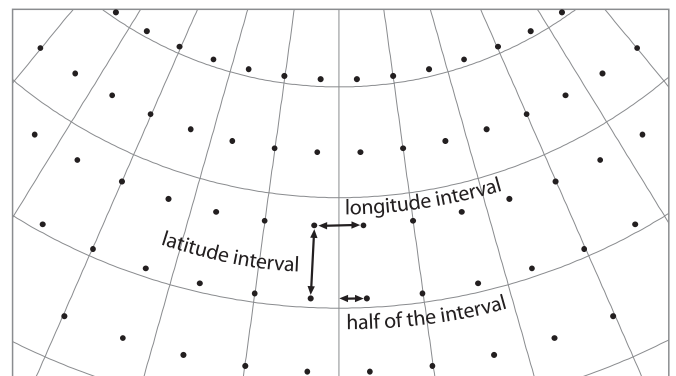


Fig. 4. An example of a regular grid of sample points with 5 rows. The longitude and latitude intervals are the same length in degrees. The central meridian is placed in-between the two central columns of points.

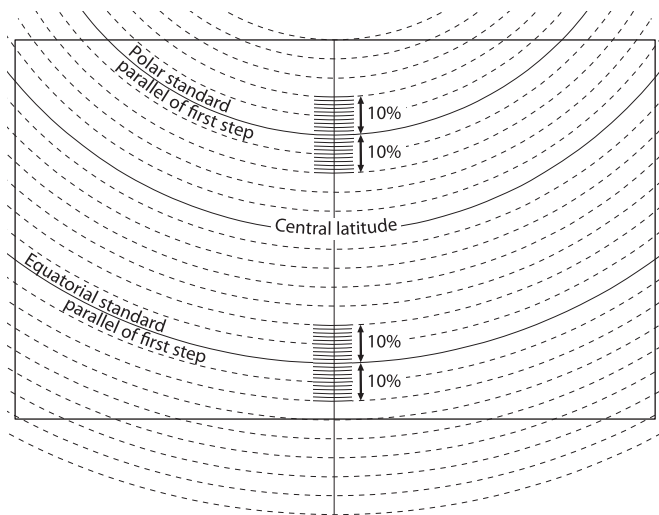


Fig. 5. Computing optimal standard parallels for the map extent for a rectangular map. Dashed parallel lines show tested parallels in the first step. Short solid black lines demonstrate the second step when 10% of the mapped central meridian length above and below the resulting parallels in the first step is analyzed again.

3.4. Computing optimal standard parallels

The optimal standard parallels were computed in two steps for each mapping scenario. In the first step, polar and equatorial standard parallels were computed for each 5% of the central meridian length (dashed parallel lines in Fig. 5). The polar parallels were tested between the maximum mapped latitude on the central meridian and the central latitude value. For the equatorial parallels, tested values ranged between the central latitude down to five standard parallels below the minimum mapped latitude on the central meridian (see Fig. 5). These extra five parallels were included in the test since some mapping scenarios with high width-to-height ratios have better distortion measures with a standard parallel below the minimum mapped latitude. For all possible combinations of standard parallels, the weighted mean error in the overall scale distortion was computed, and the combination with the smallest distortion measure was recorded. Fig. 5 demonstrates resulting standard parallels of the first step with solid black parallel lines.

In the second step, 10% of the mapped central meridian length above and below the resulting parallels was analyzed again to more accurately define the standard parallels. On Fig. 5, short solid black lines along the central meridian demonstrate the second step. The parallel interval was set at 1% instead of 5% of the central meridian length. Again, all possible combinations were tested and the one with the smallest weighted mean error in the overall scale distortion was selected as having the optimal standard parallels for the examined mapping scenario.

The methodology used for computing the optimal standard parallels was computationally expensive, and it took about four days to analyze all 3825 different mapping scenarios for one conic projection. There were three main reasons for why the computation was so expensive: (1) a large number of sample points were used to compute the distortion measure, (2) computationally expensive functions, e.g. sine, cosine, and tangent, were used to project sample points and compute numerical derivatives, and (3) there were many possible combinations for both standard parallels. A high number of sample points was required to ensure that the distortion measures were of good quality. To accelerate the computation speed, partial derivatives were analytically derived from the original projection formulas and were used instead of a numerical approximation. Appendix details the analytical

derivatives for the three conic projections used in this research. To minimize the number of possible combinations to test, the optimal standard parallels were defined in the two-step method described previously. All together, only about 200 combinations needed to be tested for each mapping scenario, instead of all 2500 possible combinations with the parallel interval set at 1% of the central meridian length.

The results of this two-step method were two standard parallels for each mapping scenario and for each of the three conic map projections. In the following steps, the latitude distance between the equatorial parallel and the minimum latitude of the mapped central meridian, and the latitude distance between the polar parallel and the maximum latitude of the mapped central meridian were computed. These distances to equatorial and polar parallels were used for the approximation of the mathematical model. Fig. 6 shows the resulting distances to the equatorial parallels and Fig. 7 shows the resulting distances to the polar parallels, both for the equidistant conic projection.

3.5. Derivation of the mathematical model

By visualizing the distances between the latitude limits of the mapped central meridian and the standard parallels (Figs. 6 and 7), it is apparent that they are changing with all three variables used to define the mapping scenarios: the length of the mapped central meridian ($\Delta\phi$), the central latitude (ϕ_c), and the width-to-height ratio of the map (α) (Fig. 2). In order to develop a model for the placement of standard parallels for conic projections, an approximation method using the least squares adjustment of indirect observations (Mikhail and Ackerman, 1976) with polynomial functions was used. The idea was to find two polynomials for each of the conic projections that would return appropriate standard parallels for the three given variables ($\Delta\phi$, ϕ_c , α). The goal was to approximate the distances with up to 6 polynomial terms for each of the standard parallels. The polynomials should have the same number of terms, and the terms should have variables with the same polynomial degrees for each conic map projection, while the polynomial coefficients could change among projections. This section presents how the final mathematical model for the standard parallels was derived.

3.5.1. Initial polynomial equations

Polynomials of varying degrees for each variable were selected and tested on how well they approximated the original values of the optimal standard parallels. In this trial-and-error process, a polynomial approximation with a minimum number of terms was determined for every standard parallel separately. To approximate distances to the equatorial parallel, a polynomial degree of two for all three variables was selected (Eq. (3)). The approximation of the distances to the polar parallel required a polynomial degree of three for the central latitude and the length of the mapped central meridian (Eq. (4)).

$$\begin{aligned} \Delta\phi_1(\alpha, \Delta\phi, \phi_c) = & (P_{1,1} + P_{1,2} \cdot \alpha + P_{1,3} \cdot \alpha^2) \cdot \\ & (P_{1,4} + P_{1,5} \cdot \Delta\phi + P_{1,6} \cdot \Delta\phi^2) \cdot \\ & (P_{1,7} + P_{1,8} \cdot \phi_c + P_{1,9} \cdot \phi_c^2) \end{aligned} \quad (3)$$

$$\begin{aligned} \Delta\phi_2(\alpha, \Delta\phi, \phi_c) = & (P_{2,1} + P_{2,2} \cdot \alpha + P_{2,3} \cdot \alpha^2) \cdot \\ & (P_{2,4} + P_{2,5} \cdot \Delta\phi + P_{2,6} \cdot \Delta\phi^2 + P_{2,7} \cdot \Delta\phi^3) \cdot \\ & (P_{2,8} + P_{2,9} \cdot \phi_c + P_{2,10} \cdot \phi_c^2 + P_{2,11} \cdot \phi_c^3) \end{aligned} \quad (4)$$

where $\Delta\phi_1$ is the distance between the equatorial parallel and the minimum latitude of the mapped central meridian, $\Delta\phi_2$ is the distance between the polar parallel and the maximum latitude of

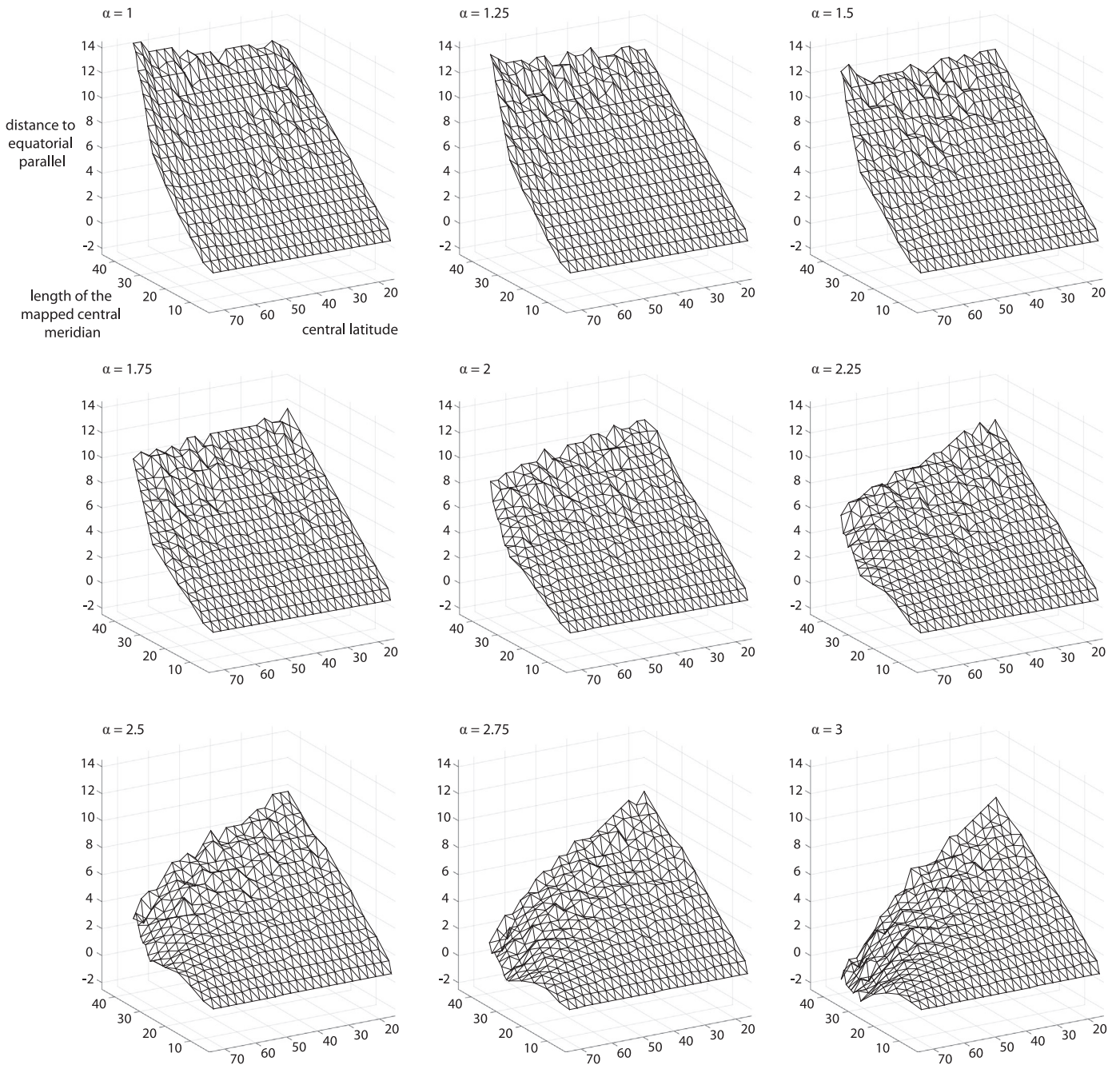


Fig. 6. Distances between the minimum latitude of the mapped central meridian and the equatorial parallels for all nine analyzed width-to-height ratios in the equidistant conic map projection. The width-to-height ratio grows from 1 at the top-left to 3 at the bottom-right.

the mapped central meridian, α is the width-to-height ratio of the map, $\Delta\phi$ is the length of the mapped central meridian in radians, ϕ_C is the central latitude, and $P_{1,1}, \dots, P_{2,11}$ are the polynomial coefficients.

3.5.2. Simplification of the polynomial equations

The mathematical model presented in Eqs. (3) and (4), would require 20 polynomial coefficients for one conic projection. The expanded version of Eq. (3), where each term in the parentheses is multiplied out by all terms in the other parentheses, consists of 27 polynomial terms; the expansion of Eq. (4) has 48 polynomial terms. This model can be simplified to make the programming of the method easier.

Before starting the simplification, the polynomials from Eqs. (3) and (4) were expanded. The simplification of each polynomial was a separate iterative process in which polynomial terms with

small contributions were removed. The iteration consisted of the following four steps:

- (1) Each polynomial term was separately removed from the function, and a new least squares adjustment was computed for all three conic projections.
- (2) For each adjustment, the residuals (the differences between the original and approximated distances to the parallel) were computed and scaled to the length of the mapped central meridian.
- (3) For each removed polynomial term, the combined reference variance for all three conic projections was computed from the scaled residuals.
- (4) The polynomial term that had the smallest combined reference variance was removed from the polynomial function.

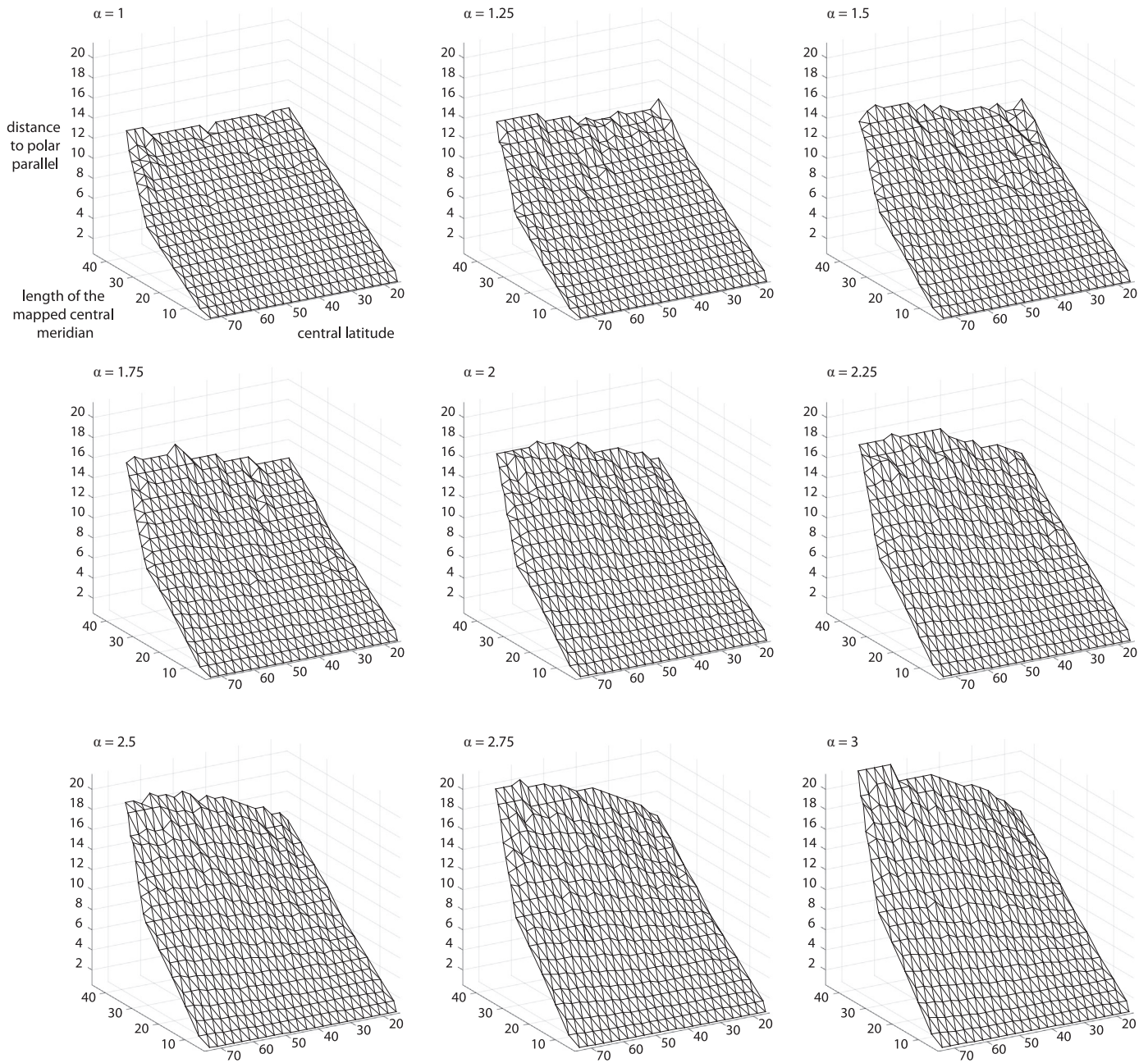


Fig. 7. Distances between the maximum latitude of the mapped central meridian and the polar parallels for all 9 analyzed width-to-height ratios in the equidistant conic map projection. The width-to-height ratio grows from 1 at the top-left to 3 at the bottom-right.

This iterative process continued until there were six or less polynomial terms left in each polynomial modeling the standard parallels. An additional measure used in this process was the reference variance for each of the conic projections and standard parallels. While removing polynomial terms, the goal was to keep all six (three for each of the two standard parallels) reference variances under 2%.

4. Results

4.1. Polynomial models for selecting standard parallels

The distances between the equatorial parallel and the minimum latitude of the mapped central meridian were approximated with a 5-term polynomial, and the distance between the polar parallel and the maximum latitude of the mapped central meridian was

approximated with a 6-term polynomial. Table 1 details the polynomial terms and their coefficient values for each of the standard parallels and conic map projections. Table 1 also details the average residuals and reference variance of the least squares adjustment for each approximation. The Albers equal-area projection has the highest average residuals and reference variance for the distances to the polar parallels and the lowest measures for the distances to the equatorial parallels. The average residuals and reference variance for the Lambert conformal conic projection are the highest for the distances to the equatorial parallels and the lowest for the distances to the polar parallels. The average residuals and reference variance for the equidistant conic projection have intermediate values.

Using the polynomial terms and their coefficients presented in Table 1, standard parallels for all three conic map projections can be determined for the northern hemisphere with Eq. (5).

Table 1
 Polynomial terms and their coefficients for computing the distances between the latitude limits of the mapped central meridian and the standard parallels. $\Delta\phi_1$ is the latitude distance to the equatorial parallels, $\Delta\phi_2$ is the latitude distance to the polar parallel, α is the width-to-height ratio of the map, $\Delta\phi$ is the length of the mapped central meridian in latitude, ϕ_C is the central latitude, $\hat{\sigma}_0^2$ is the reference variance of the least squares adjustment relative to the length of the mapped central meridian, and \bar{v} is the average of the residuals from the least squares adjustment.

Polynomial term	Albers equal-area		Equidistant		Lambert conformal	
	$\Delta\phi_1$	$\Delta\phi_2$	$\Delta\phi_1$	$\Delta\phi_2$	$\Delta\phi_1$	$\Delta\phi_2$
$\alpha^2 \cdot \Delta\phi^3 \cdot \phi_C^2$		-0.013735		-0.030964		-0.045199
$\alpha^2 \cdot \Delta\phi^2 \cdot \phi_C$	-0.038187		-0.041097		-0.045357	
$\alpha \cdot \Delta\phi^2 \cdot \phi_C^3$		-0.042567		0.0016111		0.043362
$\alpha \cdot \Delta\phi^2 \cdot \phi_C^2$	-0.12311		-0.12481		-0.12699	
$\alpha \cdot \Delta\phi^2 \cdot \phi_C$	0.066481	0.244	0.088351	0.23467	0.11504	0.22637
$\alpha \cdot \Delta\phi^3$		-0.022273		-0.013771		-0.0061132
$\Delta\phi^2 \cdot \phi_C^2$	0.21952		0.16272		0.09789	
$\Delta\phi^2 \cdot \phi_C$		-0.22285		-0.19724		-0.1766
$\Delta\phi$	0.24185	0.24137	0.23488	0.23863	0.22895	0.23604
$\hat{\sigma}_0^2$ [%]	0.9614	1.8322	1.239	1.2785	1.6904	1.0711
\bar{v} [%]	0.74004	0.94025	0.85051	0.82632	0.97691	0.78703

$$\varphi_1 = \varphi_{min} + \Delta\varphi_1 \text{ and } \varphi_2 = \varphi_{max} - \Delta\varphi_2 \tag{5}$$

$$\Delta\varphi_1 = A_1 \cdot \Delta\varphi + A_2 \cdot \Delta\varphi^2 \cdot \varphi_C^2 + A_3 \cdot \alpha \cdot \Delta\varphi^2 \cdot \varphi_C^2 + A_4 \cdot \alpha \cdot \Delta\varphi^2 \cdot \varphi_C + A_5 \cdot \alpha^2 \cdot \Delta\varphi^2 \cdot \varphi_C$$

$$\Delta\varphi_2 = B_1 \cdot \Delta\varphi + B_2 \cdot \alpha \cdot \Delta\varphi^3 + B_3 \cdot \Delta\varphi^2 \cdot \varphi_C + B_4 \cdot \alpha \cdot \Delta\varphi^2 \cdot \varphi_C + B_5 \cdot \alpha^2 \cdot \Delta\varphi^3 \cdot \varphi_C^2 + B_6 \cdot \alpha \cdot \Delta\varphi^2 \cdot \varphi_C^3$$

where ϕ_1 is the equatorial parallel, ϕ_2 is the polar parallel, ϕ_{max} is the maximum latitude of the mapped central meridian, ϕ_{min} is the minimum latitude of the mapped central meridian, α is the width-to-height ratio of the map, $\Delta\phi$ is the length of the mapped central meridian in radians, ϕ_C is the absolute value of the central latitude in radians, and $A_1 \dots A_5$ and $B_1 \dots B_6$ are the polynomial coefficients in Table 1. For the southern hemisphere, the equatorial parallel is computed by subtracting the distance $\Delta\phi_1$ from the maximum latitude ϕ_{max} . The polar parallel is computed by adding the

minimum latitude ϕ_{min} to the distance $\Delta\phi_2$.

To reduce the amount of multiplication required, the polynomial equations for the distances $\Delta\phi_1$ and $\Delta\phi_2$ can be simplified with Eqs. (6) and (7). Eq. (6) has only 7 (instead of 13) multiplications and Eq. (7) has only 11 (instead of 18) multiplications.

$$\Delta\phi_1 = \Delta\phi \cdot (A_1 + \Delta\phi \cdot \phi_C \cdot (\phi_C \cdot (A_2 + A_3 \cdot \alpha) + \alpha \cdot (A_4 + A_5 \cdot \alpha))) \tag{6}$$

$$\Delta\phi_2 = \Delta\phi \cdot (B_1 + \Delta\phi \cdot (B_2 \cdot \alpha \cdot \Delta\phi + \phi_C \cdot (B_3 + \alpha \cdot (B_4 + B_5 \cdot \alpha \cdot \Delta\phi \cdot \phi_C + B_6 \cdot \phi_C^2)))) \tag{7}$$

Figs. 8 and 9 show two examples of how the standard parallels change with the length of the mapped central meridian and the central latitude of the map. Fig. 8 is an example of the Albers equal-area projection, where the central latitude is 38.5° and the width-to-height ratio of the map is 1.6. The positions of the standard parallels vary with the length of the mapped central meridian (map extent) between 5° and 45°. This example demonstrates the change in the standard parallels when the user of a web map zooms out of a specific area at intermediate latitudes.

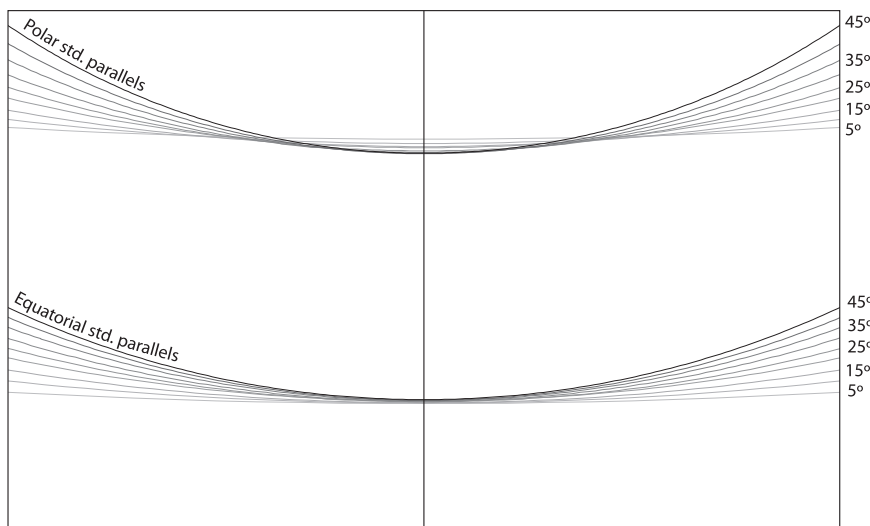


Fig. 8. The locations of standard parallels for the Albers equal-area projection, changing with the length of the mapped central meridian. The central latitude is 38.5° and the width-to-height ratio of the map is 1.6.

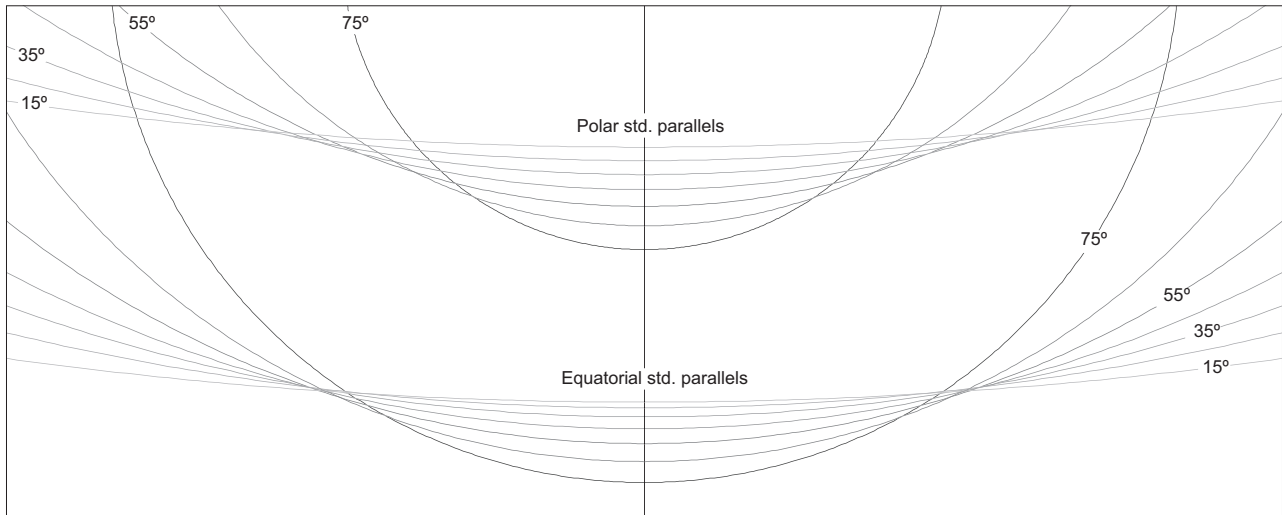


Fig. 9. The locations of the standard parallels for the Lambert conformal conic projection, changing with the central latitude of the map. The length of the mapped central meridian is 25° and the width-to-height ratio of the map is 2.5.

The locations of both standard parallels slightly change, while the displayed parallels are more curved due to the larger area on a web map.

Fig. 9 shows a more extreme example for the Lambert conformal projection, where the length of the mapped central meridian is 25° and the width-to-height ratio of the map is 2.5. The positions of the standard parallels vary with the central latitude of the map between 15° and 75°. This example demonstrates the change in the standard parallels when the user pans on a web map along the central meridian towards the pole. While the user pans closer to the North Pole, the positions of the standard parallels move further south on the map and the standard parallels become more curved.

4.2. Evaluation of the model

Two approaches were used to evaluate our polynomial models for the standard parallels. In the first approach, Deetz and Adams' (1934) and Kavrayskiy's (Maling, 1960, 1992) models were compared with the polynomial model introduced in this article. Canters and Decler's (1989) weighted mean error in the overall scale distortion is used for this analysis. The second evaluation approach compares the projected land features and the scale distortion isolines of three specific examples.

For all mapping scenarios used to approximate the polynomial models, standard parallels were determined using Deetz and Adams' (1934), Kavrayskiy's (Maling, 1960, 1992), and the polynomial (introduced in this article) models. Kavrayskiy's model uses $K = 3$ for mapped regions with square outlines and $K = 7$ for mapped regions with a larger extent in longitude. In this analysis, we followed Kavrayskiy's suggestion and the constant $K = 3$ was used for the width-to-height ratios 1 and 1.25, since they display regions with close to square outlines, and $K = 7$ was used for other width-to-height ratios, because their mapped regions have a larger extent in longitude. The weighted mean error in the overall scale distortion was then computed for every mapping scenario and the polynomial model was compared to the other two models. The percentage differences between the polynomial model and other two models were calculated. For each mapping scenario, the polynomial model resulted in a smaller weighted mean error in the overall scale distortion value. Table 2 details the averages and standard deviations for all three conic projections and both comparisons to the polynomial method.

Compared to the Deetz and Adams (1934) model, the polynomial approach improves the weighted mean error in the overall

Table 2

The minimum, maximum, average, and standard deviation of the percentage differences of the weighted mean error in the overall scale distortion for all three conic projections. The polynomial model improves the scale distortion compared to Deetz and Adams' (1934), and Kavrayskiy's (Maling, 1960, 1992) models.

Model	Projection	Min. [%]	Max. [%]	Average [%]	Std. dev. [%]
Deetz and Adams	Albers	-2.7	-28.8	-14.9	3.2
	Equidistant	-11.3	-30.9	-16.2	3.9
	Lambert	-11.1	-36.8	-17.8	5.7
Kavrayskiy	Albers	-4.7	-29.4	-18.5	6.1
	Equidistant	-2.1	-31.5	-19.4	7.0
	Lambert	-2.4	-36.5	-20.8	8.1

scale distortion between 2.7% and 28.8% for mapping scenarios in the Albers conic projection, between 11.3% and 30.9% in the case of the equidistant conic projection, and between 11.1% and 36.8% in the Lambert conic projection. On average, the weighted mean error in the overall scale distortion is improved between approximately 14.9% and 17.8% (Table 2).

The polynomial model presented in this article also improves the weighted mean error in the overall scale distortion compared to Kavrayskiy's method (Maling, 1960, 1992). The results show that the weighted mean error in the overall scale distortion improved between 4.7% and 29.4% for mapping scenarios in the Albers conic projection, between 2.1% and 31.5% in the case of the equidistant conic projection, and between 2.4% and 36.5% in the Lambert conic projection. As shown in Table 2, on average the weighted mean error in the overall scale distortion improved between 18.5% and 20.8%.

Three specific examples are used to evaluate the visual differences in projected land features and scale distortion isolines on the map: (1) the contiguous United States projected with the Lambert conic projection (Fig. 10, top), (2) Europe projected with the equidistant conic projection (Fig. 10, middle), and (3) Russia projected with the Albers equal-area conic projection (Fig. 10, bottom). For each of the examples in Fig. 10, the projected landforms and distortion lines in red are those using the polynomial model to define the standard parallels. Blue represents the other method to which the polynomial model is compared. The contiguous United States example compares the polynomial model to the parallels at 33° and 45° north, as suggested by Snyder (Snyder, 1987, p. 104). The example of Europe compares the model to the

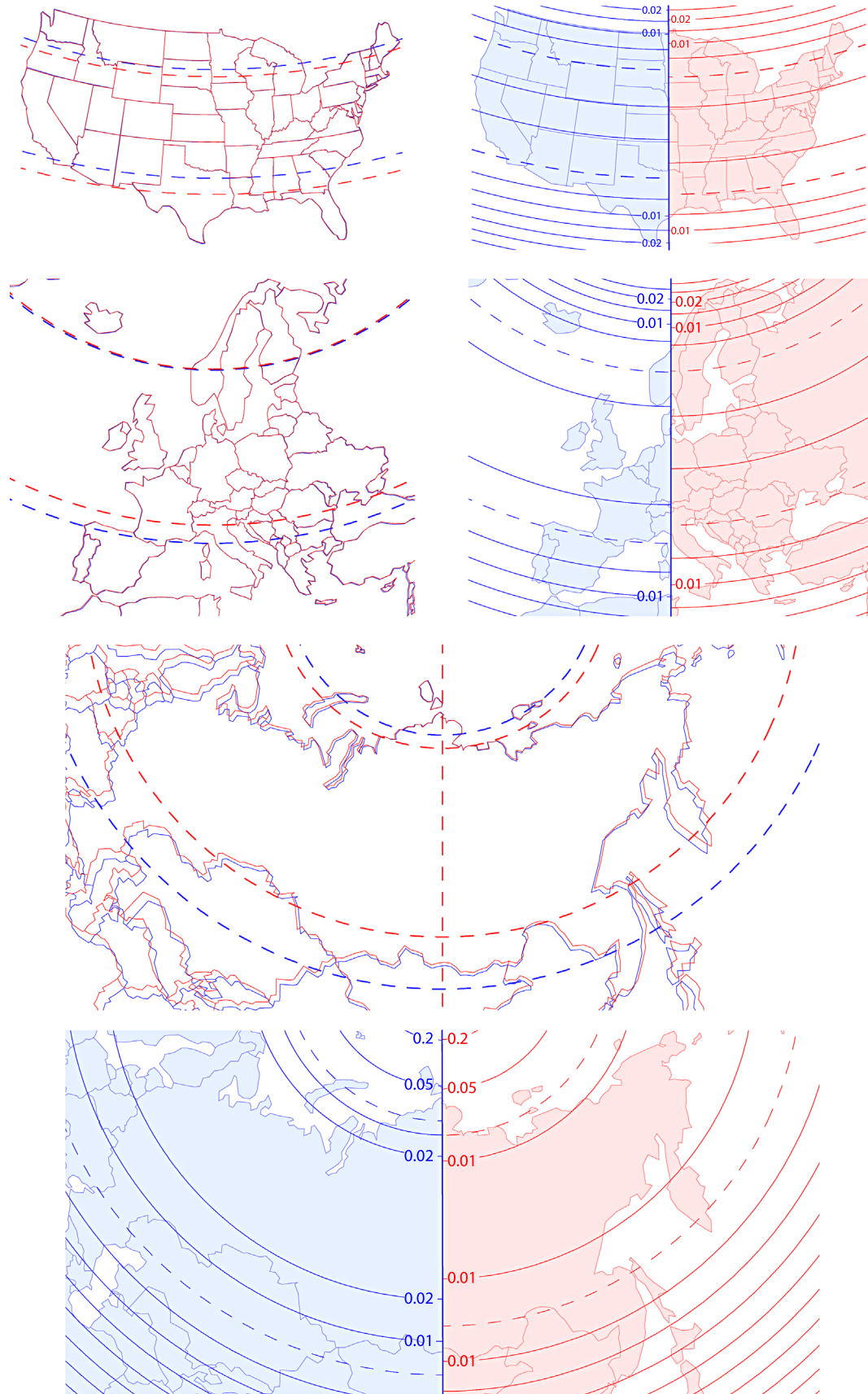


Fig. 10. Three examples showing the visual differences in projected land features and scale distortion isolines. Red shows landforms and distortion isolines with standard parallels defined using the polynomial model. Blue represents landforms and distortion isolines with the standard parallels defined using the models specified in the text. (For interpretation of the references to color in this figure legend, the reader is referred to the web version of this article.)

parallels at 43° and 62° north, as used in Esri's ArcMap projection library. The example of Russia compares the polynomial model to Deetz and Adams' (1934) approach, using the Kavrayskiy constant $K = 6$, resulting in parallels at 47° 50' and 75° 10' north.

In the case of the contiguous United States and Europe, the visual differences are very small and barely noticeable. The standard parallels defined with the polynomial model result in maps where projected land features match closely to the land features projected with standard parallels suggested by Snyder or used in Esri's projection library. Some differences can be seen when the scale distortion properties are compared. The polynomial model results in slightly larger scale distortion in peripheral areas, while the center of the map is less distorted.

The visual differences are more apparent in the example of Russia projected with the Albers equal-area conic projection. This example shows a mapping scenario with a larger geographic extent and a central latitude closer to the pole. The width-to-height ratio of the map is relatively high, about 2.06, the central latitude is 66°, and the length of the mapped central meridian is 41°. The biggest differences in the projected land features are on the peripheral parts of the map, which is the expected result. The scale distortion characteristics are similar to the other two examples – the peripheral areas have slightly greater distortion and the center of the map is less distorted. Due to the larger area being mapped, the scale distortion values are larger than the distortion values of the other two examples.

4.3. Implementation of the model

The automatic computation of standard parallels using the polynomial model can be executed in two steps. The bounding box of the geographic area to be mapped is established using the width-to-height ratio, the central latitude, and the length of the mapped central meridian, which are approximated using Eq. (8).

$$\widetilde{\Delta\phi} = \phi_{max} - \phi_{min}, \widetilde{\phi}_C = \left| \frac{\phi_{max} + \phi_{min}}{2} \right|, \widetilde{\alpha} = \frac{\Delta\phi}{\lambda_{max} - \lambda_{min}} \quad (8)$$

where $\widetilde{\Delta\phi}$ is the approximated length of the central meridian, $\widetilde{\phi}_C$ is the approximated absolute value of the central latitude, $\widetilde{\alpha}$ is the approximated width-to-height ratio of the map, ϕ_{max} is the maximum latitude of the geographic area to be mapped, ϕ_{min} is the minimum latitude of the geographic area to be mapped, λ_{max} is the maximum longitude of the geographic area to be mapped, and λ_{min} is the minimum longitude of the geographic area to be mapped.

The geographic area is then projected with the conic projection using the standard parallels defined by the approximated parameters. In cases where the approximated parameters exceed the valid range, the closest limit value can be used instead. The bounding box of the geographic area projected with a conic map projection has a fan shape. In order to include the whole projected bounding box, the mapped central meridian segment must exceed the maximum latitude of the geographic area. In the next step, a new maximum latitude (or a minimum latitude when mapping the southern hemisphere) for the mapped central meridian is determined using an inverse projection equation, and the length of the mapped central meridian and central latitude are recomputed using Eq. (8). The projected geographic bounding box does not result in the same width-to-height ratio of the map as it was approximated in the first step. A new value for the width-to-height ratio of the map is also defined from the projected geographic bounding box. Using these new parameter values, the standard parallels are defined and the geographic area is projected again. The second step can be repeated to ensure that the parameters for determining the standard parallels are defined accurately. In most cases, a third iteration is not required.

5. Conclusion

The polynomial model presented in this article extends the existing recommendations and rules of thumb for placing the standard parallels of the three most common conic projections. The major advantage of the polynomial model is that it also takes both the central latitude and the extent of the mapped area into account, which has not been the case in any of the pre-existing models. Another advantage is that this method does not assume the same model for equatorial and polar standard parallels. Both parallels are defined with different polynomials.

The polynomial equations determine the standard parallels of conic projections based on the length of the mapped central meridian, the central latitude, and the width-to-height ratio of the map. The equations have the same polynomial terms for the three conic projections. However, they have different polynomial coefficients. Using Eqs. (5)–(7), the standard parallels are computed with 11 additions and 18 multiplications per mapping scenario. Since the standard parallels are determined only once for any change of parameters, the polynomial method is fast enough for projecting data on the fly within a web mapping framework. This method can also be used in automated map projection selection tools or in GIS software.

Acknowledgments

The support of Esri, Inc. is greatly acknowledged, including valuable discussions with David Burrows, Melita Kennedy, Scott Morehouse, Dawn Wright and others. The authors would like to thank Jane E. Darbyshire from Oregon State University for editing the text of this article, as well as the anonymous reviewers for their valuable comments.

Appendix. Partial derivatives

$$\frac{\partial x}{\partial \lambda} = \rho \cdot \cos \theta \cdot n$$

$$\frac{\partial y}{\partial \lambda} = \rho \cdot \sin \theta \cdot n$$

$$\frac{\partial x}{\partial \phi} = \frac{\partial \rho}{\partial \phi} \cdot \sin \theta$$

$$\frac{\partial y}{\partial \phi} = - \frac{\partial \rho}{\partial \phi} \cdot \cos \theta$$

where for the *Albers equal-area conic projection* the variables are:

$$\frac{\partial \rho}{\partial \phi} = - \frac{\cos \phi}{n \cdot \rho}$$

$$\rho = \frac{1}{n} \cdot \sqrt{C - 2n \cdot \sin \phi}$$

$$\theta = n \cdot (\lambda - \lambda_0)$$

$$C = \cos^2 \phi_1 + 2n \cdot \sin \phi_1$$

$$n = (\sin \phi_1 + \sin \phi_2) / 2$$

where for the *Lambert conformal conic projection* the variables are:

$$\frac{\partial \rho}{\partial \phi} = - \frac{n \cdot \rho}{\sin(\pi/2 + \phi)}$$

$$\rho = \frac{F}{\tan^n(\pi/4 + \phi/2)}$$

$$\theta = n \cdot (\lambda - \lambda_0)$$

$$F = \cos \phi_1 \cdot \tan^n\left(\frac{\pi}{4} + \frac{\phi_1}{2}\right) / n$$

$$n = \frac{\ln(\cos \phi_1 / \cos \phi_2)}{\ln\left[\frac{\tan(\pi/4 + \phi_2/2)}{\tan(\pi/4 + \phi_1/2)}\right]}$$

where for the *equidistant conic projection* the variables are:

$$\frac{\partial \rho}{\partial \phi} = - 1$$

$$\rho = (G - \phi)$$

$$\theta = n \cdot (\lambda - \lambda_0)$$

$$G = \cos \phi_1 / n + \phi_1$$

$$n = (\cos \phi_1 - \cos \phi_2) / (\phi_2 - \phi_1)$$

and where for all three conic projections x and y are the projected coordinates, ϕ and λ are the latitude and longitude, λ_0 is the longitude of the central meridian, ϕ_1 is the equatorial parallel, and ϕ_2 is the polar parallel.

References

- Bugayevskiy, L.M., Snyder, J.P., 1995. *Map Projections: A Reference Manual*. Taylor & Francis, London, p. 328.
- Canter, F., 2002. *Small-scale Map Projection Design*. Taylor & Francis, London, p. 336.
- Canter, F., Declair, H., 1989. *The World in Perspective: A Directory of World Map Projections*. John Wiley and Sons, Chichester, p. 181.
- Deetz, C.H., Adams, O.S., 1934. *Elements of Map Projection with Applications to Map and Chart Construction*, 4th ed.68. U.S. Coast and Geodetic Survey Special Publication, Washington, p. 163.
- Hinks, A.R., 1912. *Map Projections*, 2nd ed. Cambridge University Press, Cambridge, p. 126.
- Hrvatini, U., 2011. Izbiranje ekvivalentne kartografske projekcije za kartiranje kontinentov (Selecting a Cartographic Equivalent Projection For Mapping Continents). University of Ljubljana, Faculty of Civil and Geodetic Engineering, Ljubljana, Slovenia, p. 93.
- Jenny, B., 2012. Adaptive composite map projections. *IEEE Trans. Vis. Comput. Graph. (Proc. Sci. Vis./Inf. Vis.)* 18 (12), 2575–2582. <http://dx.doi.org/10.1109/TVCG.2012.192>.
- Jenny, B., Patterson, T., Hurni, L., 2008. Flex Projector – interactive software for designing world map projections. *Cartogr. Perspect.* 59, 12–27. <http://dx.doi.org/10.14714/CP59.245>.
- Jenny, B., Patterson, T., Hurni, L., 2010. Graphical design of world map projections. *Int. J. Geogr. Inf. Sci.* 24 (44), 1687–1702. <http://dx.doi.org/10.1080/13658811003596101>.
- Jenny, B., Šavrič, B., Patterson, T., 2015. A compromise aspect-adaptive cylindrical projection for world maps. *Int. J. Geogr. Inf. Sci.* 29 (6), 935–952. <http://dx.doi.org/10.1080/13658816.2014.997734>.
- Maling, D.H., 1960. A review of some Russian map projections. Part II. *Emp. Surv. Rev.* 15 (116), 255–266.
- Maling, D.H., 1992. *Coordinate Systems and Map Projections*, 2nd ed. Pergamon Press, Oxford, p. 476.
- Mikhail, E.M., Ackerman, F., 1976. *Observations and Least Squares*. Harper & Row, Publishers, New York, p. 497.
- Mulcahy, K., 2000. Two new metrics for evaluating pixel-based change in data sets of global extent due to projection transformation. *Cartogr. Int. J. Geogr. Inf. Geovis.* 37 (2), 1–12. <http://dx.doi.org/10.3138/C157-258R-2202-5835>.
- Šavrič, B., Jenny, B., 2014. A new pseudocylindrical equal-area projection for adaptive composite map projections. *Int. J. Geogr. Inf. Sci.* 28 (12), 2373–2389. <http://dx.doi.org/10.1080/13658816.2014.924628>.
- Snyder, J.P., 1987. *Map Projections: A Working Manual*. US Geological Survey, Washington, DC, p. 383.